ANL-78-40

ADVANCED FUEL CELL DEVELOPMENT

Progress Report for January—March 1978

by

J. P. Ackerman, P. A. Finn, K. Kinoshita,
G. H. Kucera, J. W. Sim, and R. B. Swaroop

RETURN TO REFERENCE FILE
TECHNICAL PUBLICATIONS
DEPARTMENT

U of C-AUA-USDOE

ARGONNE NATIONAL LABORATORY, ARGONNE, ILLINOIS

Prepared for the U. S. DEPARTMENT OF ENERGY
under Contract W-31-109-Eng-38

The facilities of Argonne National Laboratory are owned by the United States Government. Under the terms of a contract (W-31-109-Eng-38) between the U. S. Department of Energy, Argonne Universities Association and The University of Chicago, the University employs the staff and operates the Laboratory in accordance with policies and programs formulated, approved and reviewed by the Association.

MEMBERS OF ARGONNE UNIVERSITIES ASSOCIATION

The University of Arizona
Carnegie-Mellon University
Case Western Reserve University
The University of Chicago
University of Cincinnati
Illinois Institute of Technology
University of Illinois
Indiana University
Iowa State University
The University of Iowa
Kansas State University
The University of Kansas
Loyola University
Marquette University
Michigan State University
The University of Michigan
University of Minnesota
University of Missouri
Northwestern University
University of Notre Dame
The Ohio State University
Ohio University
The Pennsylvania State University
Purdue University
Saint Louis University
Southern Illinois University
The University of Texas at Austin
Washington University
Wayne State University
The University of Wisconsin

NOTICE

This report was prepared as an account of work sponsored by the United States Government. Neither the United States nor the United States Department of Energy, nor any of their employees, nor any of their contractors, subcontractors, or their employees, makes any warranty, express or implied, or assumes any legal liability or responsibility for the accuracy, completeness or usefulness of any information, apparatus, product or process disclosed, or represents that its use would not infringe privately-owned rights. Mention of commercial products, their manufacturers, or their suppliers in this publication does not imply or connote approval or disapproval of the product by Argonne National Laboratory or the U. S. Department of Energy.

Printed in the United States of America
Available from
National Technical Information Service
U. S. Department of Commerce
5285 Port Royal Road
Springfield, Virginia 22161
Price: Printed Copy $4.50; Microfiche $3.00

Distribution Category:
Energy Conversion
(UC-93)

ANL-78-40

ARGONNE NATIONAL LABORATORY
9700 South Cass Avenue
Argonne, Illinois 60439

ADVANCED FUEL CELL DEVELOPMENT

Progress Report for
January—March 1978

by

J. P. Ackerman, P. A. Finn, K. Kinoshita,
G. H. Kucera, J. W. Sim, and R. B. Swaroop

Chemical Engineering Division

May 1978

Previous reports in this series

ANL-77-29	January—March 1977
ANL-77-56	April—June 1977
ANL-77-79	July—September 1977
ANL-78-16	October—December 1977

TABLE OF CONTENTS

	Page
ABSTRACT	1
SUMMARY	2
I. INTRODUCTION	3
II. ELECTROLYTE DEVELOPMENT	4
A. Physical Characterization of $LiAlO_2$ Powders	4
B. Synthesis of $LiAlO_2$	5
1. Low-Temperature Synthesis of γ-$LiAlO_2$	6
2. $LiAlO_2$ Synthesis Using Low-Cost Alumina	8
3. Future Directions	18
C. Stability of $LiAlO_2$	19
1. Physical Stability of $LiAlO_2$	19
2. Chemical Stability of $LiAlO_2$	24
III. COMPONENT DEVELOPMENT	25
A. Wet Seal Protection	25
B. Thermomechanical Testing	27
IV. CELL TESTING	29
REFERENCES	34

LIST OF FIGURES

No.	Title	Page
1.	Scanning Electron Micrograph of High-Surface-Area γ-$LiAlO_2$	8
2.	Scanning Electron Micrograph of β-$LiAlO_2$ and γ-Al_2O_3 Obtained from Heating $LiOH/Al(OH)_3$ at 725 K for 1.5 h in Air	9
3.	Scanning Electron Micrograph of β-$LiAlO_2$ and γ-Al_2O_3 Obtained from Heating $Al(OH)_3$ Impregnated with LiOH at 725 K for 2 h in Air	10
4.	Scanning Electron Micrograph of β-$LiAlO_2$ Obtained from Heating $LiOH-KOH/Al(OH)_3$ in CO_2 at 300 K for 1.5 h and 775 K for 1 h	10
5.	Scanning Electron Micrograph of β-$LiAlO_2$ Produced by Homogeneous Synthesis Method: Sample 18-3B	14
6.	Scanning Electron Micrograph of β-$LiAlO_2$ Produced by Homogeneous Synthesis Method: Sample 18-6A	16
7.	Scanning Electron Micrograph of β-$LiAlO_2$ "Coarse Flowers" Produced by Homogeneous Synthesis Method: Sample 18-6.5 A	17
8.	Scanning Electron Micrograph of β-$LiAlO_2$ Clumps Produced by Homogeneous Synthesis--Sample 18-6.5 A	18
9.	Scanning Electron Micrograph of β-$LiAlO_2$ (rods) before Heat Treatment (6000X)	20
10.	Scanning Electron Micrograph of β-$LiAlO_2$ after Heating for 112 h at 960 K in Air (6000X)	21
11.	Scanning Electron Micrograph of γ-$LiAlO_2$ Produced from Heating of β-$LiAlO_2$ for 144 h at 985 K in Air (6000X)	21
12.	Scanning Electron Micrograph of β-$LiAlO_2$ after Heating for 254 h at 945 K in $H_2/CO_2/H_2O$ (6000X)	22
13.	Sample of β-$LiAlO_2$ after 212 h at 875 K in CO_2 (6000X)	23
14.	Diagram of Cell Housings Showing Section Examined Microscopically	25
15.	Photomicrograph of Section of Anode Housing After 2628 h in Operation	26
16.	Square Cell Housing	29
17.	Schematic of Square Cell Showing Gas-Flow Pattern	30
18.	Schematic of Fuel Cell Assembly	31
19.	Square Hot-Pressing Die	33

LIST OF TABLES

No.	Title	Page
1.	Methods for the Synthesis of $LiAlO_2$	6
2.	Preparation of $LiAlO_2$ by the Reaction of Al_2O_3 and LiOH in the Presence of Li_2CO_3-K_2CO_3 Mixtures	7
3.	Synthesis of $LiAlO_2$ from Low-Cost Alumina	11
4.	Reactivity of Different Aluminas with LiOH in the Presence of Li_2CO_3-K_2CO_3	13
5.	Synthesis of $LiAlO_2$ by the Homogeneous Method	15
6.	Thermal Stability of β-$LiAlO_2$ in Presence of Li_2CO_3-K_2CO_3	20
7.	Thermal Stability of γ-$LiAlO_2$ in Presence of Li_2CO_3-K_2CO_3	23
8.	Thermomechanical Measurements on Electrolyte Tiles	28

CHEMICAL ENGINEERING DIVISION

ADVANCED FUEL CELL DEVELOPMENT

January—March 1978

by

J. P. Ackerman, P. A. Finn, K. Kinoshita,
G. H. Kucera, J. W. Sim, and R. B. Swaroop

ABSTRACT

This report describes advanced fuel cell research and development activities at Argonne National Laboratory (ANL) during the period January-March 1978. These efforts have been directed toward understanding and improvement of molten-carbonate-electrolyte fuel cell components operated at temperatures near 925 K.

The primary focus of this work has been the development of electrolyte structures which have good electrolyte retention and mechanical properties as well as long term stability, and on developing methods of synthesis amenable to mass production. The characterization of these structures, their stability and their component material is, of course, an essential part of the work. A need for very fine powders of stable $LiAlO_2$ has been identified. Several synthesis routes have been shown to be promising, and characterization capability has been upgraded.

Cell testing is essential for understanding and testing individual and collective component behavior. A more realistic cell design (10.6-cm square cells) and associated ancillaries have been put into use, replacing the older 7-cm round cells, and an economical method of wet-seal protection has been proven in cell operation.

SUMMARY

Electrolyte Development

Physical Characterization of $LiAlO_2$ Particles. Four methods of characterization--X-ray diffraction analysis, scanning electron microscopy, BET surface-area measurement, and particle-size analysis--are reviewed. The methods of sample handling used for particle-size analysis are novel, and are described in some detail.

Electrolyte Synthesis. Several new approaches to the preparation of improved $LiAlO_2$ materials were investigated. It is essential that the $LiAlO_2$ particles have and retain high surface area (small particle size) to provide the tiles with good strength and electrolyte retention. Elongated (rodlike) geometry is also desirable. Emphasis was therefore placed on the preparation of stable $LiAlO_2$ structures of small particle size and elongated shape by methods usable for mass production, and on the use of low-cost alumina as the starting materials. Three of the most attractive syntheses were (1) the heterogeneous synthesis at 775 K (500°C) of discrete particles of γ-$LiAlO_2$ having a surface area of 17 m^2/g (this material has the potential for good stability); (2) the homogeneous synthesis at ambient temperature of high-surface-area (59 m^2/g), somewhat agglomerated β-$LiAlO_2$ from low-cost alumina and (3) the heterogeneous synthesis of rodlike β-$LiAlO_2$ of fairly high surface area (13 m^2/g) from low-cost alumina. Testing of these attractive materials is just now beginning.

Stability of $LiAlO_2$

Physical Stability. Initial short-term tests on allotropically pure α-, β-, and γ-$LiAlO_2$ indicate that the γ-allotrope is stable to allotropic transformation at cell operating temperatures, and that allotropic transformation and particle growth are accelerated by the presence of air.

Chemical Stability. At a temperature of $\sim$995 K in the presence of air, $LiAlO_2$ partially decomposes to β-Li_5AlO_4. Hydrolysis of $LiAlO_2$ at 300 K is retarded by high pH. The α-allotrope is least susceptible to hydrolysis; γ-$LiAlO_2$ is most susceptible.

Component Development

Wet Seal Corrosion. Post-test analysis and coating-characterization results are presented for aluminized wet seals. The corrosion protection of the coating is excellent, but care must be taken to extend the coating somewhat beyond the actual contact area.

Thermomechanical Tile Tests. Thermal-expansion and high-temperature creep test results are presented for some seven samples. It is clear that these tests are invaluable, but insufficient characterization has been done to allow the correlation of creep measurements with tile-component properties. This work is scheduled for major expansion.

Cell Testing

A square (10.6-cm x 10.6-cm) cell design has been adopted. We believe that cells of this design yield more realistic current-collection and gas-flow properties, and their somewhat larger size provides a more realistic electrolyte environment than did the previous small, round cells. The new cell design, initial operation of square cells, and related equipment are discussed.

I. INTRODUCTION

The advanced fuel cell studies at Argonne National Laboratory (ANL) are part of the DOE Second Generation Fuel Cell Program. The goal of this DOE program is the earliest possible introduction of high-efficiency generating systems based on molten-carbonate fuel cells, which have the capability of operating on coal or other fuels. At the present state of development, the primary thrust of the program is directed to development of the fuel cell itself.

A molten carbonate fuel cell consists of a porous metal anode (presently nickel or an alloy of nickel), a porous nickel oxide cathode, an electrolyte structure which separates the anode and cathode and conducts only ionic current between them, and appropriate metal housings or, in the case of stacks of cells, intercell separator plates. The cell housings (or separator plates) bear upon the electrolyte structure to form a seal between the environment and the anode and cathode gas compartments. The electrolyte structure, which is commonly called a "tile," is a composite structure of solid $LiAlO_2$ particles and a mixture of alkali metal carbonates which are liquid at the cell operating temperature of 925 K. At the anode, hydrogen and carbon monoxide in the fuel gas react with carbonate ion from the electrolyte to form carbon dioxide and water, giving up electrons to the external circuit. At the cathode, carbon dioxide and oxygen react and accept electrons from the external circuit to re-form carbonate ion, which is conducted through the electrolyte to the anode. In a practical cell stack, CO_2 for the cathode would be obtained from the anode exhaust.

The ANL contribution to the program is intended to provide understanding of cell behavior and to develop improved components and processes. More improvements are needed in the electrolyte tile than in any other single component. For this reason, electrolyte development is receiving special attention at ANL. Characterization of tile properties and the relation of the properties to tile behavior in cells is of major importance. Determination of the stability of tile materials is also of high priority.

Operation of cells is required for assessment of the behavior of tiles and other components and for understanding of the performance and life-limiting mechanisms at work within the cell. Cell operation is, of course, coupled with a diagnostic effort and a materials-development effort, with the aim of developing cells of adequate performance and longevity for realistic component testing.

II. ELECTROLYTE DEVELOPMENT

A. Physical Characterization of $LiAlO_2$ Powders

A major emphasis of the ANL research and development effort on molten carbonate fuel cells has centered on the preparation and characterization of $LiAlO_2$ used in electrolyte tiles. In the past, the physical characterization of the $LiAlO_2$ powders has been done primarily by the use of X-ray diffraction analysis* and scanning electron microscopy. More recently, measurements of particle size and surface area have been incorporated as routine tools for the characterization of $LiAlO_2$ powders. The additional information obtained by the latter two measurement techniques will be useful in relating the physical properties of the $LiAlO_2$ powders and the performance of these materials in electrolyte tiles.

The surface areas of $LiAlO_2$ samples are measured with a Model 2100D Orr Surface-Area Pore-Volume Analyzer (Micromeritics Instrument Corporation) using N_2 as the adsorbate at liquid nitrogen temperature. Powder samples of $LiAlO_2$ mixed with 55 wt % Li_2CO_3-K_2CO_3 (62 mol % Li_2CO_3-38 mol % K_2CO_3) are treated with an acetic acid/acetic anhydride solution to remove the alkali carbonates, washed with methanol and dried prior to the surface area measurement. The amount of N_2 adsorbed on the $LiAlO_2$ sample is measured at relative pressures P/P_o (P is the partial pressure of N_2 and P_o is the saturation pressure of N_2 at liquid nitrogen temperature) of 0.05-0.3 and the surface area is calculated from these measurements by the BET† equation.

The $LiAlO_2$ particle size and size distribution are determined with a Celloscope (Particle Data Laboratory, Elmhurst, Illinois) particle analyzer, which calculates the particle size from a conductometric measurement.‡ This technique involves the measurement of the resistivity change (ΔR) of an electrolyte due to the presence of insulator particles such as $LiAlO_2$. As the $LiAlO_2$ particles suspended in an electrolyte pass through an orifice, ΔR is measured by electrodes on each side of the orifice. If the resistivity of the particles is considerably greater than that of the electrolyte, then ΔR is generally obtained for particles having sizes in the range from 2 to 40% of the orifice diameter. The concentration of particles in the electrolyte is made low enough to insure a high probability that only one particle at a time is measured as it passes through the orifice. Typically, the conductometric measurements are made on about 200,000 particles and the data are stored in a computer for later analysis. Since ΔR is proportional to the particle volume, the particle diameter calculated by the computer is the equivalent diameter for a sphere having the same volume as the particle.

---

*All X-ray diffraction analyses described in this report were performed by B. S. Tani, Analytical Chemistry Laboratory, ANL.

†Brunauer, Emmett and Teller.

‡Measurements performed at Particle Data Laboratories, Elmhurst, IL.

The particle-size measurements required an electrolyte that was suitable for dispersing the $LiAlO_2$ powder and was compatible with the conductometric measurement. The electrolyte generally used in the particle-size analyzer (saline solution) was not suitable because of the reactivity of $LiAlO_2$ toward H_2O. An obvious alternative was glacial acetic acid/acetic anhydride (70:30 vol %), the solution used in our procedure for isolating $LiAlO_2$, but the electrical conductivity of this material was too low. However, the addition of 4 wt % Li_2CO_3 to 100 ml of the acetic acid/acetic anhydride solution increased the electrical conductivity of the electrolyte sufficiently so that meaningful measurements of ΔR could be obtained. The samples of $LiAlO_2$ prepared in reactant mixtures containing Li_2CO_3-K_2CO_3 do not require the addition of Li_2CO_3 prior to the conductometric measurement, because the amount of alkali carbonates originally present in the sample provides adequate conductivity. Thus, the procedure selected allows direct analysis of the $LiAlO_2$ particles without prior isolation from alkali carbonates and thereby minimizes losses due to sample handling.

The allotropic form of $LiAlO_2$ (α, β, or γ) is identified by X-ray diffraction analysis using a Norelco X-ray unit. Powder samples of $LiAlO_2$ are placed in 0.02-cm-dia glass capillaries and exposed to 45-kV, filtered Cu K_α X-rays (15 mA) in a 114.6-mm powder diffraction camera. Typically, the exposure time to the X-rays is about 3 h.

Scanning electron microscopy is used to determine the shape of the $LiAlO_2$ particles. Samples are prepared for SEM analysis by first ultrasonically dispersing the $LiAlO_2$ powder in methanol and then placing a drop of the dispersed $LiAlO_2$ on a specimen holder. After evaporation of the methanol, a thin (20 nm) coating of gold is evaporated onto the $LiAlO_2$ particles. The samples are examined in a scanning electron microscope (Model JSM 35, manufactured by Japanese Electron Optics Laboratory), usually at magnifications of 6000X; however, magnifications of 300 to 15000X have been used.

B. Synthesis of $LiAlO_2$

The objective of this part of the ANL effort is to develop methods for synthesizing $LiAlO_2$ that provide electrolyte structures with high strength and conductivity as well as good electrolyte retention. In addition, these methods must be amenable to the mass production of electrolyte structures. Several methods of synthesizing $LiAlO_2$ that appear to yield desirable products for use in electrolyte structures are currently being investigated.

Table 1 briefly outlines the methods of synthesizing $LiAlO_2$ that were examined during this quarter. These methods can be divided into two general classifications--heterogeneous and homogeneous. In the methods classified as heterogeneous, $LiAlO_2$ is formed by heating (1) a physical mixture of LiOH and alumina powders or (2) alumina powder impregnated with LiOH (ANL-77-29, p. 4). In the homogeneous method, alumina powder is dissolved in KOH or KOH-LiOH and the $LiAlO_2$ is obtained by precipitation from LiOH solution directly or by addition to methanol, respectively.

Table 1. Methods for the Synthesis of $LiAlO_2$

Synthesis Method	Reactant Mixing Technique	Reactant Composition	Sample Treatment
Heterogeneous	Physical mixture	LiOH/alumina[a]	Heat in air
Heterogeneous	Impregnated	LiOH/alumina[a]	Heat in air
Heterogeneous	Physical mixture	LiOH/alumina[a]/ Li_2CO_3-K_2CO_3	Heat in air
Heterogeneous	Impregnated	LiOH-KOH/alumina[a]	Heat in CO_2
Homogeneous	Dissolution	$Al(OH)_3$ dissolved in LiOH-KOH solution	Spray alkali solution into methanol
Homogeneous	Dissolution	$Al(OH)_3$ dissolved in KOH solution	Spray KOH solution into LiOH solution

[a]The alumina was Al_2O_3, $Al(OH)_3$ or AlOOH.

1. Low-Temperature Synthesis of γ-$LiAlO_2$

Our results indicate that γ-$LiAlO_2$ is the most stable allotrope of $LiAlO_2$ for molten carbonate fuel-cell applications (ANL-77-29, p. 14). However, γ-$LiAlO_2$ is generally obtained by heating samples at high temperatures (>950 K), where undesirable particle growth occurs; the resulting large particles of γ-$LiAlO_2$ do not possess the electrolyte-retention properties required in electrolyte tiles. Accordingly, a method for producing γ-$LiAlO_2$ at lower temperatures was sought. Semenov[1] reported that in the presence of Li_2CO_3 the rate of transformation of α- to γ-$LiAlO_2$ at 975-1075 K increased as the amount of Li_2CO_3 was increased (called "mineralizing effect"); these results suggested that the formation of γ-$LiAlO_2$ could be carried out at lower temperatures, where particle growth would not be significant.

Experiments were therefore designed to synthesize high-surface-area γ-$LiAlO_2$ at relatively low temperatures by using Li_2CO_3-K_2CO_3 in the reaction mixture of LiOH and alumina to provide the environment for the so-called "mineralizing effect." The amount of Li_2CO_3-K_2CO_3 (62 mol % Li_2CO_3-35 mol %) added was sufficient to yield an electrolyte containing 55 wt % alkali carbonates after reaction to form $LiAlO_2$. The experiments were conducted with Degussa, Inc., Type C γ-Al_2O_3 because we have had the most experience with this material. A Hungarian patent[2] has claimed a procedure for producing γ-$LiAlO_2$ by heating mixtures of LiOH, Li_2CO_3, Na_2CO_3 and γ-Al_2O_3 or $Al(OH)_3$ at 965 K for 10-12 h in air. However, we believe that a lower synthesis temperature is required to produce high-surface-area γ-$LiAlO_2$.

Table 2 summarizes the conditions in our experiments to optimize the synthesis of γ-$LiAlO_2$. The samples were prepared by physically mixing LiOH and γ-Al_2O_3 (Degussa, Type C), then adding sufficient Li_2CO_3-K_2CO_3 to yield an electrolyte containing 55 wt % carbonates after reaction to form

$LiAlO_2$. Heating this mixture in air at 625 K for 24 h produced only the β-$LiAlO_2$ allotrope; heating at 675 K for 20.5 h or 725 K for 1.5 h, however, yielded a major phase of γ-$LiAlO_2$ and some β-$LiAlO_2$. At 775 K the product was predominantly γ-$LiAlO_2$ after 1.5 h; at 825 K, a very minor amount of α-$LiAlO_2$ was also produced. (SEM analysis showed that clump-shaped particles were produced in all samples listed in Table 2.) These results suggested that 775 K is probably the optimum reaction temperature for the synthesis of γ-$LiAlO_2$ from a mixture of LiOH, γ-Al_2O_3, Li_2CO_3 and K_2CO_3.

Table 2. Preparation of $LiAlO_2$ by the Reaction of Al_2O_3 and LiOH in the Presence of Li_2CO_3-K_2CO_3 Mixtures[a]

Sample No.	Temperature, K	Time, h	$LiAlO_2$ Phases
45	625	23	β-$LiAlO_2$
48	675	20.5	β-$LiAlO_2$ (major) γ-$LiAlO_2$ (major)
62	725	1.5	β-$LiAlO_2$ (major) γ-$LiAlO_2$ (major)
74	775	1.5	γ-$LiAlO_2$ (major) β-$LiAlO_2$ (possible minor)
81	825	1.5	γ-$LiAlO_2$ (major) β-$LiAlO_2$ (minor) α-$LiAlO_2$ (very minor)

[a]Initial molar composition: 2.0 LiOH + 1.0 γ-Al_2O_3 + 1.0 Li_2CO_3 + 0.6 K_2CO_3; the γ-Al_2O_3 used in all experiments was Degussa, Type C.

Effort was then directed toward producing γ-$LiAlO_2$ of high surface area by reaction of LiOH and γ-Al_2O_3 in the presence of carbonate. Heating the mixture at 775 K for 2 h in air was followed by a second heat treatment step at 975 K for 16 h in CO_2 to ensure complete conversion of γ-Al_2O_3 to γ-$LiAlO_2$. X-ray diffraction analysis confirmed that γ-$LiAlO_2$ was the only allotrope present after the second heat treatment; SEM analysis showed that the γ-$LiAlO_2$ particles were of submicrometer size ($\sim$0.2 μm) and were in the shape of irregular bipyramids (see Fig. 1). On the basis of the estimated average particle size of 0.2 μm and the assumption of approximately spherical particles, the calculated surface area is 11.5 m^2/g. This value agrees reasonably well with the BET surface area measurement by nitrogen adsorption, namely 17 m^2/g. We have concluded that γ-$LiAlO_2$ of reasonably high surface area can be obtained by the two-step heat treatment of LiOH, γ-Al_2O_3, Li_2CO_3, and K_2CO_3 mixtures at 775 and 975 K. In the near future, electrolyte tiles incorporating γ-$LiAlO_2$ particles of submicrometer size will be tested in 10.6-cm-square cells.

Fig. 1. Scanning Electron Micrograph of High-Surface-Area γ-$LiAlO_2$ (produced from $LiOH/\gamma$-Al_2O_3/Li_2CO_3-K_2CO_3 heated at 775 K for 2 h and 975 K for 16 h)

2. $LiAlO_2$ Synthesis Using Low-Cost Alumina

a. Heterogeneous Methods

Studies to examine the feasibility of preparing $LiAlO_2$ from low-cost alumina were continued in experiments with hydrated alumina, $Al(OH)_3$, type H-705.* This alumina costs \$0.57/kg (\$0.26/lb) which is about one-seventh of the cost of Degussa γ-Al_2O_3. Technical data published by the manufacturer indicates that the average particles size of $Al(OH)_3$ is about 0.5 μm, a size considerably larger than the average particle size of Degussa γ-Al_2O_3 ($\sim$0.02 μm). However, the average particle size of the H-705 $Al(OH)_3$ is smaller than that of other low-cost aluminas (ALCOA F-1, C-33), which we have used previously to synthesize $LiAlO_2$.

The experimental conditions for $LiAlO_2$ synthesis from $Al(OH)_3$ are summarized in Table 3 along with results of X-ray and SEM analyses. The starting materials were prepared by physically mixing LiOH and $Al(OH)_3$ (sample 90) and by impregnating $Al(OH)_3$ with LiOH (sample 111A) or LiOH-KOH (sample 114). In all three experiments, the major product was β-$LiAlO_2$.

---

*A product of the Aluminum Company of America (ALCOA).

Analysis by SEM of a sample obtained from a physical mixture of LiOH and $Al(OH)_3$ (sample 90) after heating at 725 K for 1.5 h showed a mixture of clump- and platelet-shaped particles of submicrometer size (Fig. 2). In contrast, $Al(OH)_3$ impregnated with LiOH (sample 111A) heated to 725 K for 2 h yielded a mixture of clump- and rod-shaped particles (Fig. 3). The rod-shaped particles were $\sim$0.4 μm in diameter and $\sim$2 μm in length, while the clump-shaped particles were $\sim$1 μm in diameter. This is the first time we have synthesized rod-shaped particles of β-$LiAlO_2$ by heat treatment of a sample of alumina powder impregnated with LiOH only. Previously, rod-shaped particles of β-$LiAlO_2$ were obtained only by treatment of samples of alumina (γ-Al_2O_3, γ-AlOOH) impregnated with both LiOH and KOH. To test the reproducibility of the procedure, the experiment was repeated, with essentially identical results.

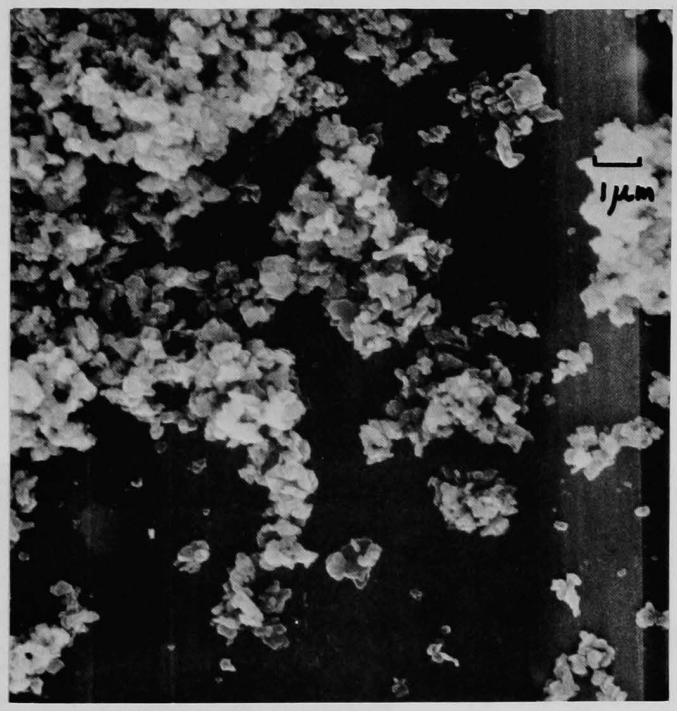

Fig. 2. Scanning Electron Micrograph of β-$LiAlO_2$ (major phase) and γ-Al_2O_3 (possible minor) Obtained from Heating LiOH/$Al(OH)_3$ at 725 K for 1.5 h in Air (sample 90, Table 3)

The electron micrograph in Fig. 4 clearly shows that rod-shaped particles can be produced by the CO_2 treatment of $Al(OH)_3$ impregnated by LiOH and KOH (sample 114). The rod-shaped particles of β-$LiAlO_2$ are about 0.4 μm in diameter and about 1.5 μm in length. The dimensions of these particles are similar to those of rod-shaped particles of β-$LiAlO_2$ obtained with precursors of $Al(OH)_3$, ALCOA C-33 (ANL-77-79, p. 4) and γ-AlOOH, ALCOA F1 (ANL-78-16, p. 6) and are somewhat smaller than those obtained from γ-Al_2O_3,

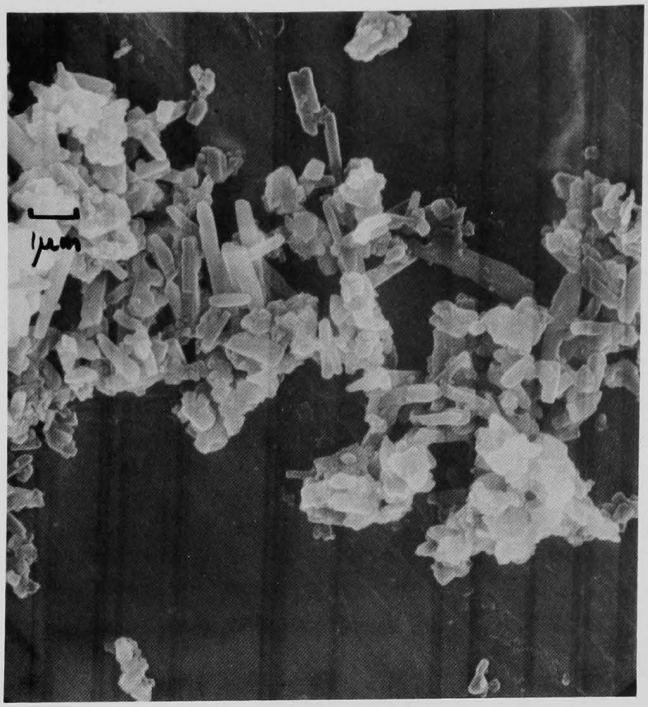

Fig. 3.

Scanning Electron Micrograph of β-$LiAlO_2$ (major phase) and γ-Al_2O_3 (very minor) Obtained from Heating $Al(OH)_3$ Impregnated with LiOH at 725 K for 2 h in Air (sample 111A, Table 3)

Fig. 4.

Scanning Electron Micrograph of β-$LiAlO_2$ Obtained from Heating LiOH-KOH/$Al(OH)_3$ in CO_2 at 300 K for 1.5 h and 775 K for 1 h (sample 114, Table 3).

Table 3. Synthesis of $LiAlO_2$ from Low-Cost Alumina

Sample No.	Reactant Composition[a]	Temp., K	Time, h	Gas Environment	X-ray Analysis	SEM Analysis
90	$LiOH/Al(OH)_3$	725	1.5	air	β-$LiAlO_2$ (major) γ-Al_2O_3 (possible minor)	clumps, platelets
111A	$LiOH/Al(OH)_3$	725	2.0	air	β-$LiAlO_2$ (minor) γ-Al_2O_3 (very minor)	clumps, rods
114	$LiOH-KOH/Al(OH)_3$	300	1.5	CO_2		
		775	1.0	CO_2	β-$LiAlO_2$	rods

[a]Molar composition: for 90 and 111A, 1.0 LiOH + 1.0 $Al(OH)_3$; for 114, 1.9 LiOH + 0.7 KOH + 0.8 $Al(OH)_3$. $Al(OH)_3$ in all samples, ALCOA H-705 hydrated alumina.

Degussa Type C (ANL-77-29, p. 11). The BET surface area of sample 114 was 13 m^2/g. In comparison, the surface area of rod-shaped particles of β-$LiAlO_2$ obtained by CO_2 treatment of Degussa γ-Al_2O_3 impregnated by LiOH and KOH was 5 m^2/g. The low surface area of the latter sample was expected since these rod-shaped particles had average dimensions of $\sim$0.7-μm diameter and $\sim$4-μm length. Furthermore, the average particle diameter was computed to be 0.96 μm, again indicating a low surface area for the rod-shaped particles of β-$LiAlO_2$ obtained with a precursor of Degussa γ-Al_2O_3.

The results in Table 2 showed that a physical mixture of LiOH, γ-Al_2O_3 (Degussa, Type C), Li_2CO_3 and K_2CO_3 heated to 775 K for 1.5 h in air produced a major phase of γ-$LiAlO_2$. On the other hand, experimental results presented in the last quarterly report (ANL-78-16, p. 9) showed that physical mixtures of LiOH, γ-AlOOH (ALCOA, F1), Li_2CO_3 and K_2CO_3 heated at 775 K for 1.5 h yielded only a minor phase of γ-$LiAlO_2$ and a major phase of γ-Al_2O_3. These results indicate that the reaction rate of γ-AlOOH with LiOH in physical mixtures containing Li_2CO_3 and K_2CO_3 was lower than that of γ-Al_2O_3 (Degussa, Type C) with LiOH in the presence of Li_2CO_3 and K_2CO_3.

During the past quarter, physical mixtures containing LiOH, $Al(OH)_3$ (ALCOA, H-705), K_2CO_3, and Li_2CO_3 were heat treated to determine if the reaction rate of LiOH and $Al(OH)_3$ was also low relative to that of LiOH and γ-Al_2O_3 (Degussa, Type C) in the presence of Li_2CO_3-K_2CO_3. The X-ray analysis data obtained on the products after heat treatments at 725 and 775 K for different times are given in Table 4. Also included in the table for reference purposes are the X-ray data obtained with starting materials of γ-Al_2O_3 (Degussa Type C) and γ-ALOOH (ALCOA F1); after heating at 775 K. The results, summarized in Table 4, show that the reaction of LiOH with $Al(OH)_3$ or γ-AlOOH at 775 K requires more than 1.5 h to obtain complete conversion to $LiAlO_2$; however, γ-Al_2O_3 is completely converted in 1.5 h at 775 K. It appears that these samples containing $Al(OH)_3$ or γ-AlOOH are first converted to γ-Al_2O_3 which then reacts with LiOH to form $LiAlO_2$. Only when the heating times are prolonged, as with sample 110, is a major $LiAlO_2$ phase formed.

b. Homogeneous Methods

The homogeneous methods summarized in Table 1 offer several attractive features for the synthesis of $LiAlO_2$. The need for a fine particle size of Al_2O_3 is eliminated in the homogeneous method since the alumina is dissolved in an alkaline solution; therefore, low-cost alumina of relatively large particle size can be used as the starting material. Furthermore, the $LiAlO_2$ is formed by rapid precipitation from solution, a procedure which generally produces high-surface-area powders.

This method also has disadvantages, however. The dissolution of the alumina is accomplished by the use of a strong alkaline solution such as KOH. The synthesis of quantities as small as $\sim$15 g of $LiAlO_2$ requires the use of moderately large volumes (1-1.5 L) of liquids which must be rapidly and thoroughly mixed. The maximum yield of $LiAlO_2$ powder by this method appears to be limited by the solubility of $LiAlO_2$. An increase in the amount of $LiAlO_2$ in solution decreases the amount of $LiAlO_2$ powder separated from the liquid phase.

Table 4. Reactivity of Different Aluminas with LiOH in the Presence of Li_2CO_3-K_2CO_3[a]

Sample No.	Alumina Phase	Alumina Manufacturer (Type)	Reaction Temp., K	Reaction Time, K	X-ray Analysis
74	γ-Al_2O_3	Degussa (C)	775	1.5	γ-$LiAlO_2$ (major) β-$LiAlO_2$ (possible minor)
75	γ-AlOOH	ALCOA (F1)	775	1.5	γ-Al_2O_3 (major) γ-AlOOH (medium) β-$LiAlO_2$ (possible minor)
98	$Al(OH)_3$	ALCOA (H-705)	725	1.5	γ-Al_2O_3
110	$Al(OH)_3$	ALCOA (H-705)	725	22	β-$LiAlO_2$ (major) unidentified amorphous phase
109	$Al(OH)_3$	ALCOA (H-705)	775	1.5	γ-Al_2O_3 (major) β-$LiAlO_2$ (minor) γ-$LiAlO_2$ (very minor)
113	$Al(OH)_3$	ALCOA (H-705)	775	3.5	unidentified amorphous phase

[a]Molar composition of starting material: 1.0 LiOH + 0.5 Al_2O_3 [1.0 AlOOH or 1.0 $Al(OH)_3$] + 1.0 Li_2CO_3 + 0.6 K_2CO_3.

The homogeneous methods of synthesizing high-surface-area $LiAlO_2$ that have been examined are summarized in Table 5, along with the results. In one method, ∿25 g $Al(OH)_3$ was dissolved in a solution containing 39 g KOH and 140 cm^3 of 14N NH_4OH at ∿370 K. The solution was cooled at 275 K and stirred vigorously while a second solution containing 11.8 g LiOH dissolved in 150 cm^3 of ∿7N NH_4OH at room temperature was added by spraying as a fine stream. Initially NH_4OH was added to decrease the solubility of $LiAlO_2$; however, the presence of NH_4OH was found to increase the rate of precipitation of $LiAlO_2$ significantly. Immediately upon contact of the two solutions, a somewhat gelatinous-appearing precipitate began to form. The precipitate was separated by centrifugation and heat treated at 725 K in air for 1.5 h. After treatment with acetic acid/acetic anhydride, the $LiAlO_2$ was collected on a 0.08-μm nucleopore filter. This method of isolation minimizes lossess due to handling the fine particulate material.

The X-ray diffraction analysis of this product (18-3B) indicated that only β-$LiAlO_2$ was present. A scanning electron micrograph of the sample (Fig. 5) shows that the particles were generally cube-shaped and <1 μm in size. The BET surface area of the β-$LiAlO_2$ sample was ∿19 m^2/g.

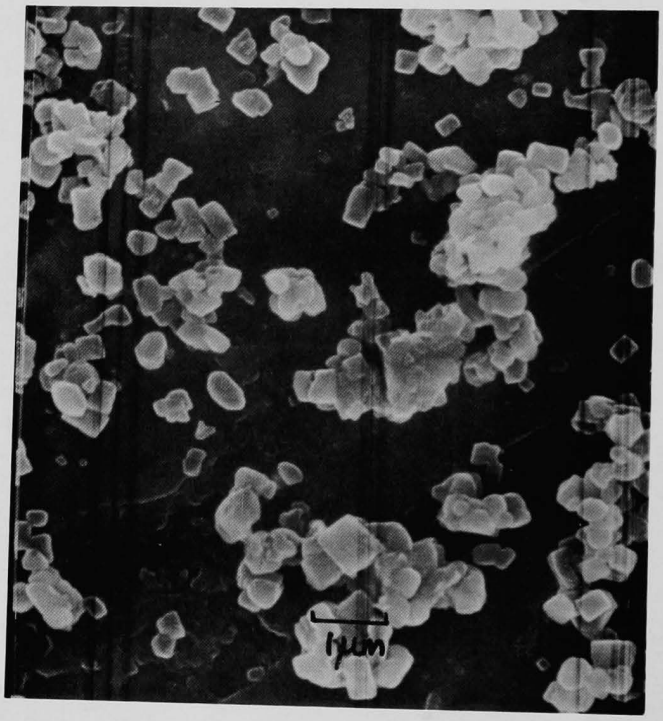

Fig. 5. Scanning Electron Micrograph of β-$LiAlO_2$ Produced by Homogeneous Synthesis Method: Sample 18-3B

In the second method, ∿2/g $Al(OH)_3$ was dissolved in a solution of 42 g KOH and 200 cm^3 H_2O at ∿370 K. Then an ambient-temperature solution of 8.7 g LiOH in 140 cm^3 H_2O was added rapidly to the $Al(OH)_3$-KOH solution. A small amount of precipitate began to form slowly upon the addition of the

Table 5. Synthesis of $LiAlO_2$ by the Homogeneous Method

Sample Identification	Starting Solutions[b]		$LiAlO_2$[a]		BET Surface Area m^2/g
	(1)	(2)	Phase	Particle Shape	
18-3B	$Al(OH)_3$ dissolved in KOH-NH_4OH	LiOH-7N NH_4OH	β	cubes	19
18-6A	$Al(OH)_3$ dissolved in KOH-LiOH	methanol	β	flower-like	59
18-6.5A	$Al(OH)_3$ dissolved in KOH-LiOH	none	β	clumps and coarse flower-like particles	7.8

[a]The precipitated $LiAlO_2$ was heat-treated at 725 K for 1.5 h in air.

[b]$Al(OH)_3$ H-705, obtained from ALCOA.

LiOH solution. About 75% of the combined LiOH-$Al(OH)_3$-KOH solution was sprayed as fine droplets into vigorously stirred, cold methanol (275 K). Copious quantities of a precipitate formed immediately, with the amount increasing as more of the reactants were introduced. The purpose of the methanol was to provide a "sink" for the water present in the aqueous alkaline solution and to decrease the solubility of the $LiAlO_2$ formed in solution. (This technique has been used by Jaeger and Miller[3] to prepare high-surface-area $MgAl_2O_4$.)

The gelatinous precipitate was separated by centrifugation, heat treated at 725 K in air for 1.5 h, washed with acetic acid/acetic anhydride, and collected by filtration as described earlier. The X-ray diffraction analysis of this product (18-6A) indicated that β-$LiAlO_2$ was formed. A scanning electron micrograph of the product, shown in Fig. 6, revealed unusual-shaped particles that can best be described as resembling tightly packed flower blossoms several micrometers in size. The very high BET surface area of this sample (59 m^2/g) indicates that the β-$LiAlO_2$ particles are probably agglomerates of smaller structures (the "petals" of the "blossoms").

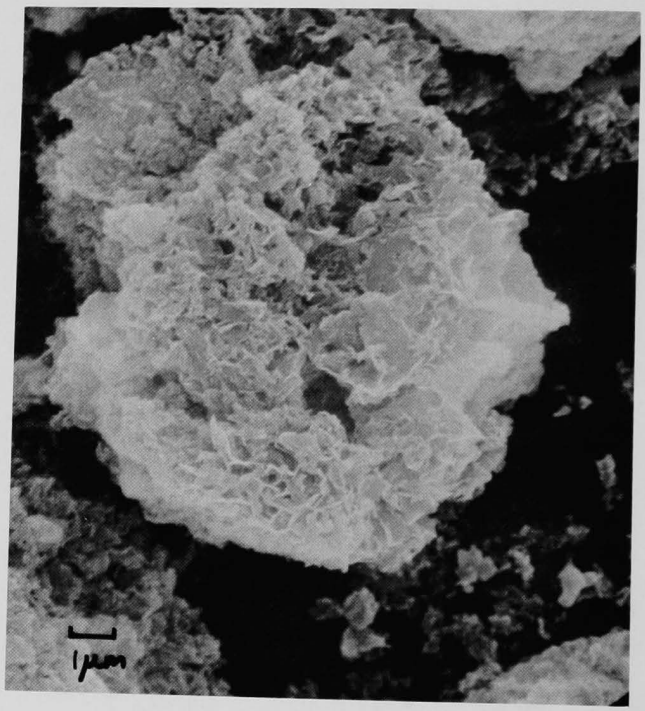

Fig. 6. Scanning Electron Micrograph of β-$LiAlO_2$ Produced by Homogeneous Synthesis Method: Sample 18-6A

The remaining 25% of the LiOH-$Al(OH)_3$-KOH solution was allowed to stand at ambient temperature for ∿15 h. During this time, a precipitate was slowly formed. Although a considerable amount of

precipitate had formed in the first 4 h, precipitation continued with time. The latter precipitate appeared dense and granular. After the liquid phase was removed by centrifugation, the precipitate was heat-treated in air at 725 K for 1.5 h, washed with acetic acid/acetic anhydride solution, and collected by filtration. The X-ray diffraction analysis of the precipitate (sample 18-6.5 A) showed only the presence of β-$LiAlO_2$. The scanning electron micrographs showed that the sample consisted of a mixture of coarse flower-like particles >5 μm in size (Fig. 7) and clumps (Fig. 8) ranging from 1 to 5 μm in size. The BET surface area of this material was 7.8 m^2/g.

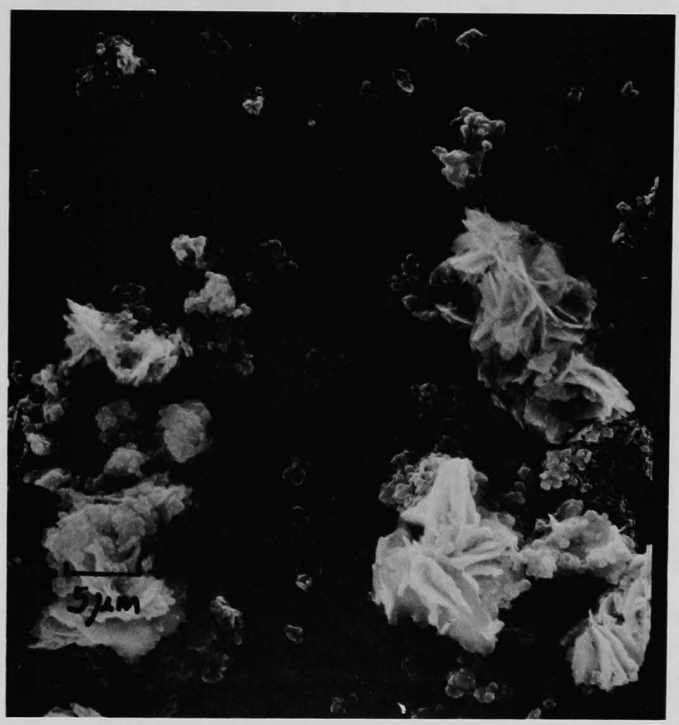

Fig. 7. Scanning Electron Micrograph of β-$LiAlO_2$ "Coarse Flowers" Produced by Homogeneous Synthesis Method: Sample 18-6.5 A

The two methods in which β-$LiAlO_2$ was precipitated rapidly appear promising as methods for producing high-surface-area $LiAlO_2$. Precipitation from a LiOH-$Al(OH)_3$-KOH-NH_4OH solution produced submicrometer-size particles with well-defined shapes; however, the surface area was no greater than that of the γ-$LiAlO_2$ sample discussed in Section B.1. On the other hand, synthesis by precipitation from a LiOH-KOH-$Al(OH)_3$ methanol solution produced β-$LiAlO_2$ particles with a high surface area but with irregular particle shapes and large agglomerate sizes. Further experiments are planned to evaluate the reproducibility of the method for producing the high-surface-area β-$LiAlO_2$. In addition, the experimental parameters will be varied to determine the optimum conditions for synthesizing $LiAlO_2$ by the homogeneous method.

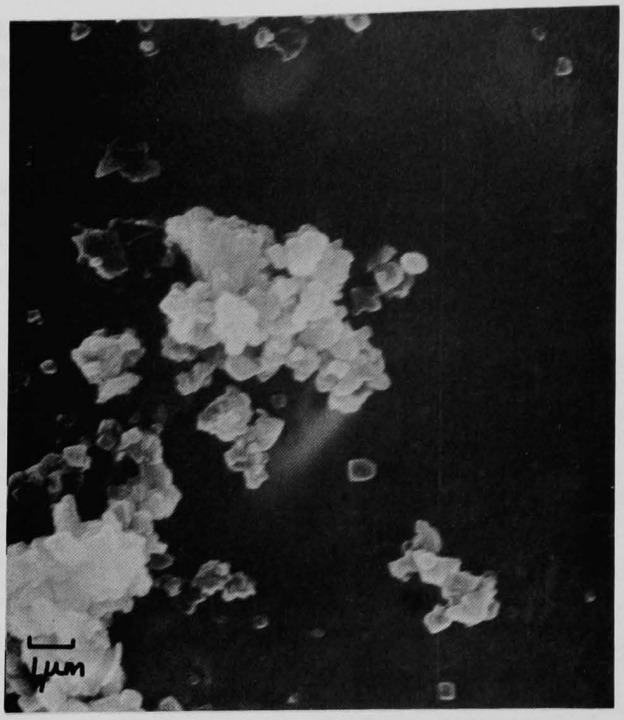

Fig. 8. Scanning Electron Micrograph of β-$LiAlO_2$ Clumps Produced by Homogeneous Synthesis: Sample 18-6.5 A

3. Future Directions

During this quarter we have prepared $LiAlO_2$ powders by a variety of synthesis methods. With the use of particle-size analyses and BET surface-area measurements to complement X-ray diffraction and SEM analyses, we are now able to obtain a more complete physical characterization of the $LiAlO_2$ samples. The BET surface-area measurements have clearly shown that we can synthesize $LiAlO_2$ powders with surface areas varying by one order of magnitude ($\sim$5 to 59 m^2/g for β-$LiAlO_2$). Furthermore, SEM has shown that $LiAlO_2$ can be prepared in different particle shapes, several of which appear to be unique to the homogeneous methods of synthesis.

Effort will be continued to develop synthesis methods for obtaining high-surface-area $LiAlO_2$. In particular, we will investigate the following syntheses: (1) the experimental conditions necessary for obtaining γ-$LiAlO_2$ from physical mixtures of low-cost alumina, LiOH, Li_2CO_3 and K_2CO_3; (2) the experimental conditions necessary for obtaining rod-shaped particles of β-$LiAlO_2$ with high surface area (>13 m^2/g); and (3) a detailed examination of homogeneous synthesis methods, with the aim of developing procedures for preparing high-surface-area $LiAlO_2$ without the use of methanol. Testing of tiles produced from the most promising $LiAlO_2$ products or selected mixtures of these products will, of course, be continued in operating cells and by thermophysical measurements (*e.g.*, thermal expansion, high temperature creep).

C. Stability of $LiAlO_2$

1. Physical Stability of $LiAlO_2$

The electrolyte-retention properties of tiles are dependent on density, size distribution, shape, and surface area of the particulate $LiAlO_2$ in the tile. It is necessary, therefore, to determine the effects of temperature and gas environment on the stability of the shape, size distribution, surface area and allotropic form of the $LiAlO_2$ particles.

Although some long-term tests were initiated early in the program, the general approach is to evaluate gross effects with short tests, and to follow these with appropriate tests of materials held for progressively longer periods of time at selected conditions of temperature and gas composition. All samples are characterized before and after heat treatment by X-ray analysis. Scanning electron micrographs, particle-size analyses, and surface-area determinations are obtained when needed.

The experiments described below were performed by heating mixtures of 45 wt % β- or γ-$LiAlO_2$ and 55 wt % Li_2CO_3-K_2CO_3 (0.62/0.38 mole ratio) at temperatures ranging from 875 to 1110 K. Similar experiments with α-$LiAlO_2$ are in progress and will be reported at a later date.

a. Tests with β-$LiAlO_2$

The conditions and results of stability tests with β-$LiAlO_2$ are given in Table 6. The β-$LiAlO_2$ used for all the experiments (see Fig. 9) consisted of small rods with a low surface area. A particle-size analysis of this material indicated that it had a relatively sharp distribution curve with a maximum at 1.2 μm.

Previous tests with this β-$LiAlO_2$ (ANL-77-56, p. 8) indicated that at 925 K, 2400 h of heating in air had no effect on the stability of this allotropic form; however, the maximum in the distribution curve obtained from a particle-size analysis increased to 1.8 μm, indicating that particle growth had occurred. At 960 K, β-$LiAlO_2$ heated for 112 h in air remained as β-$LiAlO_2$; Fig. 10 shows that although the rods are still present, they are twice the size of those in the original sample. In addition, larger species, which could be termed elongated bipyramids, are forming. When heating was continued for an additional 240 h at 960 K, the β-$LiAlO_2$ was completely converted to γ-$LiAlO_2$. Complete conversion occurred in a shorter time, 144 h, when the sample was heated at 985 K; a scanning electron micrograph of this sample is shown in Fig. 11. The particle size has increased markedly, with bipyramidal particles 20 μm in diameter being common.

Heating β-$LiAlO_2$ in an $H_2/CO_2/H_2O$ environment for 2400 h at 925 K (ANL-77-56, p. 8) produced no change in allotropic form. A particle size-analysis of that sample indicated that the size distribution was essentially identical to that of the original sample. No conversion of β-$LiAlO_2$ to γ-$LiAlO_2$ occurs in 254 h at 945 K; however, small (<1 μm) bipyramidal-shaped particles are present among the rod-shaped particles (see Fig. 12). One might expect that continued heating would result in the conversion of β-$LiAlO_2$ to γ-$LiAlO_2$, perhaps in 800 h. When β-$LiAlO_2$ is heated at 975 K for 107 h in $H_2/CO_2/H_2O$ complete conversion of β-$LiAlO_2$ to γ-$LiAlO_2$ occurs.

Table 6. Thermal Stability of β-$LiAlO_2$ in Presence of Li_2CO_3-K_2CO_3[a]

Expt. No.	Conditions: Temp., K	Conditions: Time, hr	Conditions: Gas	Final Products (X-ray Analysis)
---	925	2400	air	β-$LiAlO_2$
108-82	960	112	air	β-$LiAlO_2$
108-102	960	352	air	γ-$LiAlO_2$
108-73	985	144	air	γ-$LiAlO_2$
---	925	2400	$H_2/CO_2/H_2O$	β-$LiAlO_2$
108-80	945	254	$H_2/CO_2/H_2O$	β-$LiAlO_2$
108-44	975	67	$H_2/CO_2/H_2O$	γ-$LiAlO_2$ (major) β-$LiAlO_2$ (major)
108-50	975	107	$H_2/CO_2/H_2O$	γ-$LiAlO_2$
108-92	875	212	CO_2	β-$LiAlO_2$
108-94	925	212	CO_2	β-$LiAlO_2$
---	925	530	CO_2/air[b]	β-$LiAlO_2$
---	975	100	CO_2/air[b]	γ-$LiAlO_2$

[a] 55 wt % Li_2CO_3-K_2CO_3 (0.68/0.38 mole ratio).

[b] CO_2 passed over sample in air-atmosphere furnace.

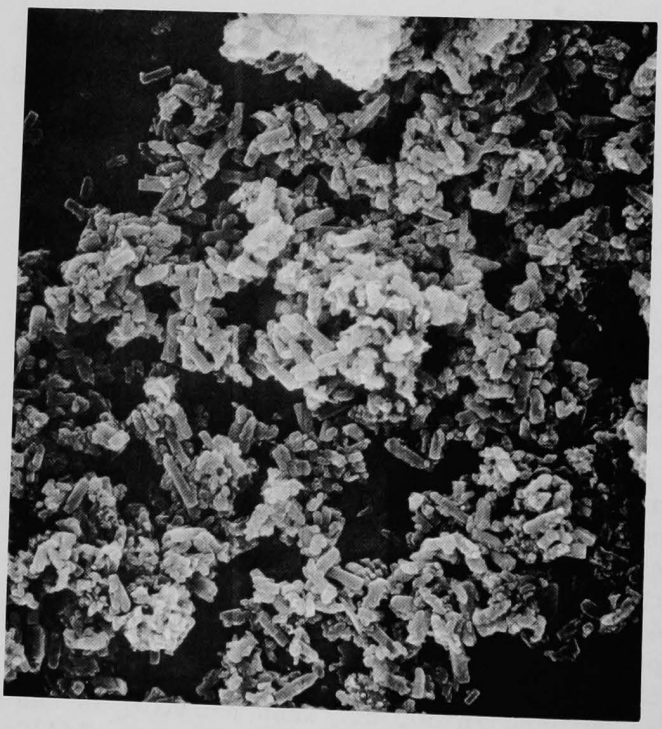

Fig. 9.

Scanning Electron Micrograph of β-$LiAlO_2$ (rods) before Heat Treatment (6000X)

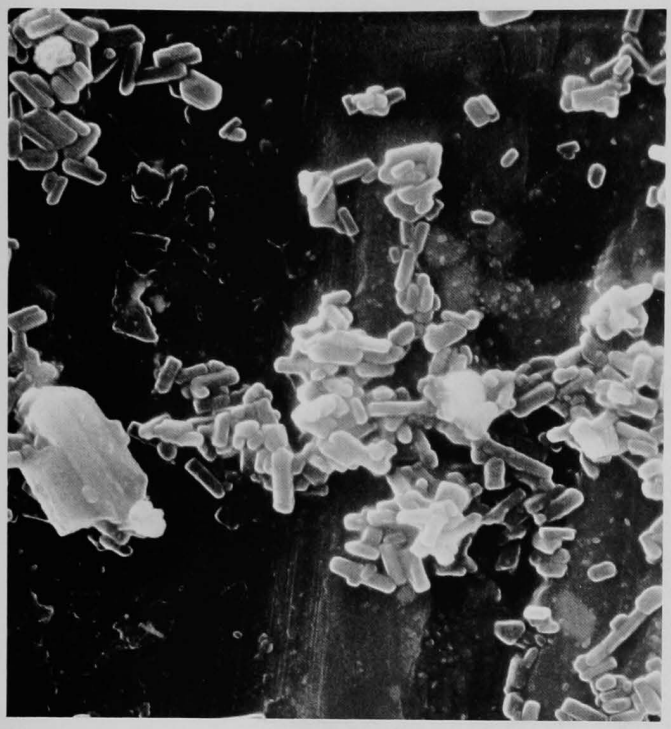

Fig. 10.

Scanning Electron Micrograph of β-$LiAlO_2$ after Heating for 112 h at 960 K in Air (6000X)

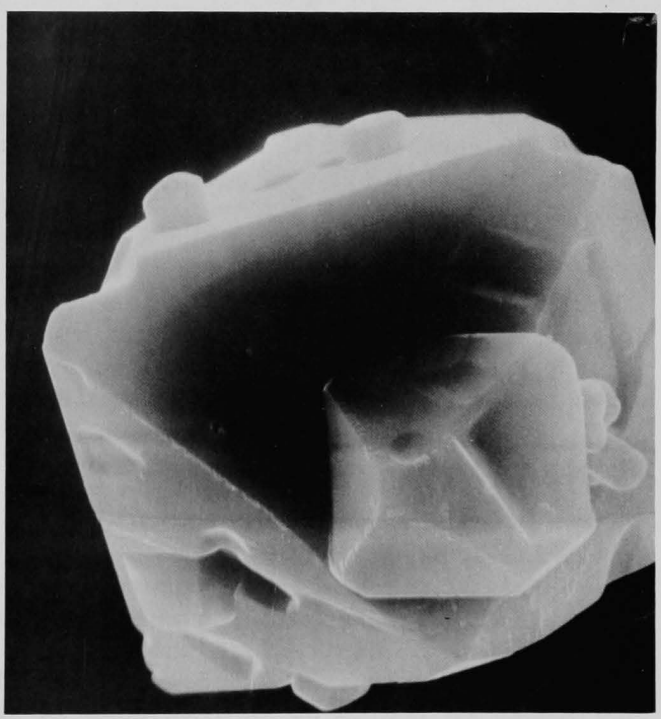

Fig. 11.

Scanning Electron Micrograph of γ-$LiAlO_2$ Produced from Heating of β-$LiAlO_2$ for 144 h at 985 K in Air (6000X)

Fig. 12. Scanning Electron Micrograph of β-$LiAlO_2$ after Heating for 254 h at 945 K in $H_2/CO_2/H_2O$ (6000X)

Transformation of β-$LiAlO_2$ to γ-$LiAlO_2$ in a CO_2/air environment occurs upon heating at 975 K for 100 h (ANL-77-29, p. 15). The particle size distribution of the heat-treated species had a broad maximum centered between 5 and 10 μm, with an appreciable number of particles >10 μm. This contrasts sharply with the distribution of original material, in which a narrow maximum was found near 1.2 μm. Prolonged heating at temperatures less than 925 K does not change the form of the β-$LiAlO_2$. Figure 13 shows that although the rod-shaped particles are for the most part unchanged, other species are forming, as indicated by the elongated rods and the bipyramidal-shaped structures.

At the operating temperature of the cell, 925 K, the β-$LiAlO_2$ should be stable in allotropic form for relatively short periods (<1000 h) regardless of gaseous environment; however, our present results indicate that particle growth will occur. The greatest change may be found in the area of the wet seal if the $LiAlO_2$ is exposed to an air environment. These data therefore argue for blanketing the exterior of fuel cell stacks with a CO_2-rich gas.

b. Tests with γ-$LiAlO_2$

Stability experiments with γ-$LiAlO_2$ are summarized in Table 7. The γ-$LiAlO_2$ samples used in these experiments were of various particle sizes but all were of bipyramidal shape with a low surface area (high-surface-area γ-$LiAlO_2$ has only recently been made). In air at 1110 K, γ-$LiAlO_2$ begins to decompose to β-Li_5AlO_4 in less than 24 h. The formation of this species is to be avoided during cell operation; therefore, care must be taken to control temperature excursions.

Table 7. Thermal Stability of γ-$LiAlO_2$ in Presence of Li_2CO_3-K_2CO_3[a]

Expt. No.	Conditions: Temp., K	Conditions: Time, h	Conditions: Gas	Final Products (X-Ray Analysis)
108-101	960	352	air	γ-$LiAlO_2$
108-38	1110	24	air	γ-$LiAlO_2$ (major) β-Li_5AlO_4 (minor)
108-93	875	212	CO_2	γ-$LiAlO_2$
108-95	925	212	CO_2	γ-$LiAlO_2$
108-91	975	15	CO_2	γ-$LiAlO_2$

[a] 55 wt % Li_2CO_3-K_2CO_3 (0.62/0.38 mole ratio).

Fig. 13. Sample of β-$LiAlO_2$ after 212 h at 875 K in CO_2 (6000X)

We plan to conduct examinations by SEM of the products formed after heat-treating high-surface-area γ-$LiAlO_2$, with the aim of determining the extent and rate of particle growth as a function of temperature, time, and gas environment. Future stability tests will also be conducted for longer time periods ($\sim$2400 h) on samples of α-, β-, and γ-$LiAlO_2$ of high surface area. The particle growth and the change in surface area will be monitored as a function of time.

2. Chemical Stability of $LiAlO_2$

In connection with the development of analytical techniques, the relative stabilities of α-, β-, and γ-$LiAlO_2$ in water and 12M HCl were reported previously (ANL-77-16, pp. 13-16). Recent experiments with aqueous 12M KOH indicate that α-, β-, and γ-$LiAlO_2$ can be recovered after 2 h of exposure, the γ-$LiAlO_2$ being recovered nearly quantitatively. The hydrolysis of α-, β-, and γ-$LiAlO_2$ is dependent on pH with γ-$LiAlO_2$ being most susceptible to hydrolysis in neutral or acidic solutions, β-$LiAlO_2$ less susceptible, and α-$LiAlO_2$ relatively inert.

III. COMPONENT DEVELOPMENT

A. Wet Seal Protection

In previous reports (ANL-77-56, p. 6; ANL-77-79, pp 12-14), we discussed a method of protecting the wet seal area of the anode housing from corrosion. The method involved flame-spraying aluminum onto the wet seal to a depth of ∿50-70 μm and heating (in vacuo or in helium) to 1275 K for ∿30 min to form a diffused layer between the aluminum and the Type 316 stainless steel cell housings. Both cell housings (anode and cathode) were coated, although corrosion of the cathode housing is generally not very severe. We reported (ANL-77-79, pp 12-14) our visual observations that corrosion did not occur in the area covered by the protective aluminum coating. Corrosion did occur in unprotected areas, however.

During the past quarter, we examined microscopically a section of the anode housing that had been used for a total of 2628 h in Cells CS-1, -2, -3, -5, and 7. A diagram of the section examined, as it relates to the overall cell configuration, is shown in Fig. 14. A photomicrograph of the

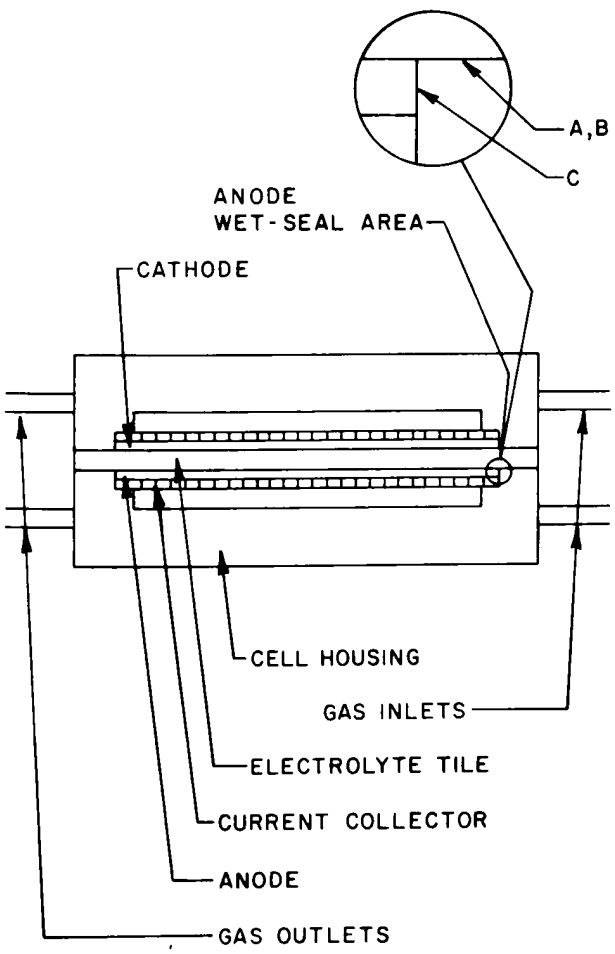

Fig. 14.

Diagram of Cell Housings Showing Section Examined Microscopically

(A, B, and C identify locations of areas A, B, and C in Fig. 15).

section is shown in Fig. 15. This photomicrograph confirms our previous observation that corrosion is undetectable in areas covered by the protective aluminum coating. A dense layer (∿30-μm thick) of oxidized aluminum (layer A in Fig. 15) covers the surface of the wet seal. The cracks

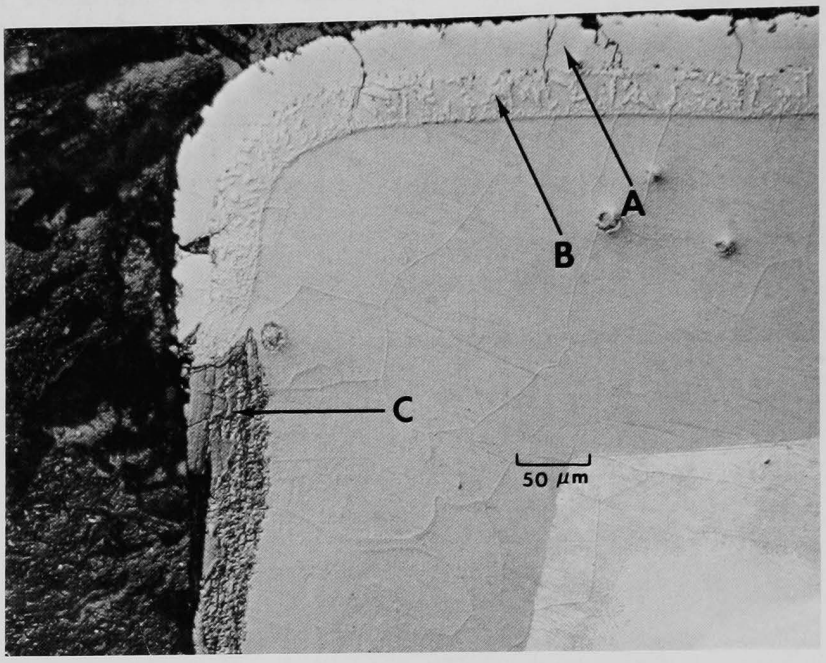

Fig. 15. Photomicrograph of Section of Anode Housing after 2628 h Operation (see also Fig. 18)

A. Oxidized aluminum layer
B. Diffused aluminum layer
C. Corrosion product at edge of electrode compartment

in layer A probably resulted from cutting and polishing of the specimen. Below layer A is a diffused layer of aluminum compounds (layer B in Fig. 15, ∿30-μm thick), which adheres to the Type 316 stainless steel cell housing. The protective aluminum coating is clearly intact; corrosion is limited to those areas of the housing which were not covered by the aluminum coating, namely, the external face of the housing and the portion of the electrode compartment immediately adjacent to the wet seal (area C in Figs. 14 and 15). Contact of the alkali carbonates with these (corroded) areas occurs when the carbonates creep out of the electrolyte tile and over the surface of the cell housings. Corrosion is unusually severe in this case because of the poor electrolyte retention of some of the experimental tiles used.

A new design of cell housing (discussed in Section IV) extends the area protected by the coating process. The external faces of the cell housings have been covered, and the coating has been extended into the electrode compartment, but not into the current-collection area. We believe that these measures will further improve corrosion resistance of the cell housings, but that they represent "overkill" in terms of practical hardware. To date, a single test cell (Cell SQ-1, 184 h) has showed no visible corrosion.

B. Thermomechanical Testing

Thermal expansion and high-temperature creep measurements were made on seven tile samples (see Table 8) using the quartz thermomechanical test rig previously described (ANL-77-56, p. 13). The measurement and interpretation of thermal expansion coefficients is straightforward. The correlation of high-temperature creep behavior with the measurable properties of the tile component, the history of the tile, as well as tile density and other measurable tile properties, is fairly complex, however, and no adequate theories of correlation exist.

It has, of course, been possible to correlate unacceptable cell performance and rapid high-temperature creep with a narrow $LiAlO_2$ particle-size distribution and large mean particle size, as in samples SC-19 and SC-20. Moreover, most of the creep has occurred fairly rapidly, *i.e.*, within 100 h after reaching the creep test temperature of 925 K.

Because of the importance of these tests for tile evaluation and eventually for stack design, we have constructed three test rigs, and will place a great deal more emphasis on thermomechanical tile testing and correlation of thermomechanical test results with other measurable tile and $LiAlO_2$ properties.

Table 8. Thermomechanical Measurements on Electrolyte Tiles

Pellet	Electrolyte Sample No.	$LiAlO_2$ Allotrope (particle shape)	Carbonate Content		Pellet Thickness, mm	Stress, kPa	α_t,[b] 10^6 K^{-1}	Instantaneous Creep (%)[c] at ~765 K	Average Creep Rate at 923 K,[c] 10^6 h^{-1}	Creep Measurement Period, h
			wt %	vol %[a]						
SC 18	134AF	α-$LiAlO_2$ (clumps)	50	63	6.3	70	12	-1.6	-80	200
SC 24	92-99	α-$LiAlO_2$ (clumps)	55	68	4.6	83	24	-0.13	-450	200
SC 22	92-99	α-$LiAlO_2$ (clumps)	55	68	6.3	86	22	-0.45	-870	80
SC 21	92-64	α-$LiAlO_2$ (clumps)	60	72	6.3	86	17	-8.3	-500	200
SC 19	98-6	β-$LiAlO_2$ (rods)	55	62	6.3	86	15	Crept instantaneously at 765 K		
SC 20	98-6	β-$LiAlO_2$ (rods)	55	62	5.9	86	12	Crept instantaneously at 765 K		
SC 23	92-101A	γ-$LiAlO_2$ (bipyramids)	55	62	6.8	86	19	-7	-115	20
SC 25	98-18	(50% α + β) (clump/rods)	55	62	6.4	86	16	-29	Did not creep further at 925 K up to 50 h	
SC 26	98-22	(80 % α + β) (clumps/rods)	55	62	6.4	86	19	-28	Did not creep further at 925 K up to 50 h	

[a] at 925 K.

[b] Thermal expansion coefficient measured between 300 to 755 K.

[c] % of original thickness.

[d] Average creep rate = $(\Delta\ell/\ell)/\Delta t$ for the period.

IV. CELL TESTING

We have designed and tested a square (10.6 x 10.6 cm) cell. The modifications incorporated into the new cell design were based on our operating experience with the round cells of the CS-series (ANL-77-56, pp 5-9; ANL-77-79, pp 9-14). The new design and its advantages are discussed below. The first test of the new cell design is also discussed.

A photograph of the square cell housing is shown in Fig. 16, and a schematic drawing in Fig. 17. The overall cell assembly is shown in Fig. 18. The anode and cathode housings are identical, and are made of Type 316 stainless steel. The tube that travels around the perimeter of the housing is used to preheat the reactant gas to operating temperature before it enters the electrode compartment. Inside the cell housing is a manifold, which ensures that gas distribution is uniform along the length of the entrance slot. This manifold is illustrated in Fig. 17. After emerging from the entrance slot, reactant gas travels along the gas channels to the exit slot, which is also connected to a manifold inside the housing (see Fig. 17). From this manifold, the gas leaves the cell via the straight gas exhaust tube. The housings were flame-sprayed with aluminum for corrosion protection; the areas covered by the protective coating appear as a light grey color in Fig. 16.

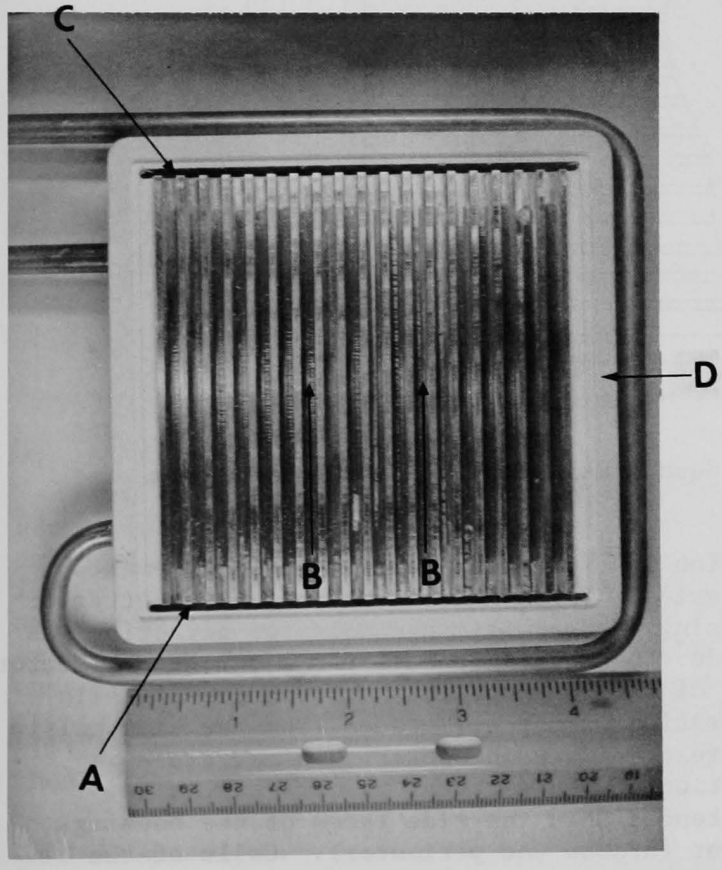

Fig. 16.

Square Cell Housing (10.6 x 10.6 cm)

A. Gas entrance slot
B. Gas channels
C. Gas exit slot
D. Wet seal area (light grey color is the area covered by protective aluminum)

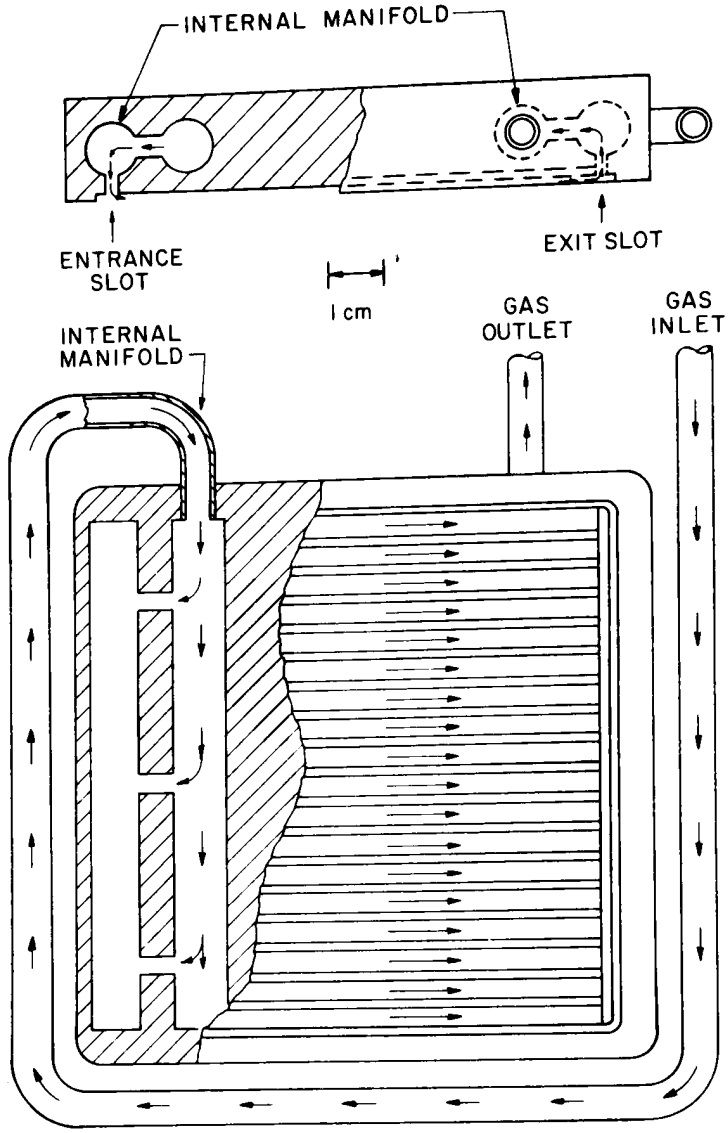

Fig. 17. Schematic of Square Cell Showing Gas-Flow Pattern

This square cell configuration incorporates a number of improvements over the round cells of the CS-series. First, gas distribution is better controlled. The square cell housing has specific channels for directing gas flow to all areas of the electrode. Second, support for the current collector and electrode is improved. Lack of this support in the CS-series of cells caused cell failure, due to separation of the electrodes from the electrolyte tile. Third, preheating of the reactant gas to operating temperature is more efficient. Finally, protection of the wet seal is more extensive. The aluminum coating has been extended down the side faces of the housings and into the electrode compartment (around the perimeter). Cells of the CS-series corroded in these areas only because the aluminum coating was not present. These improvements should result in improved cell performance and in longer usable life for test hardware and for individual cells.

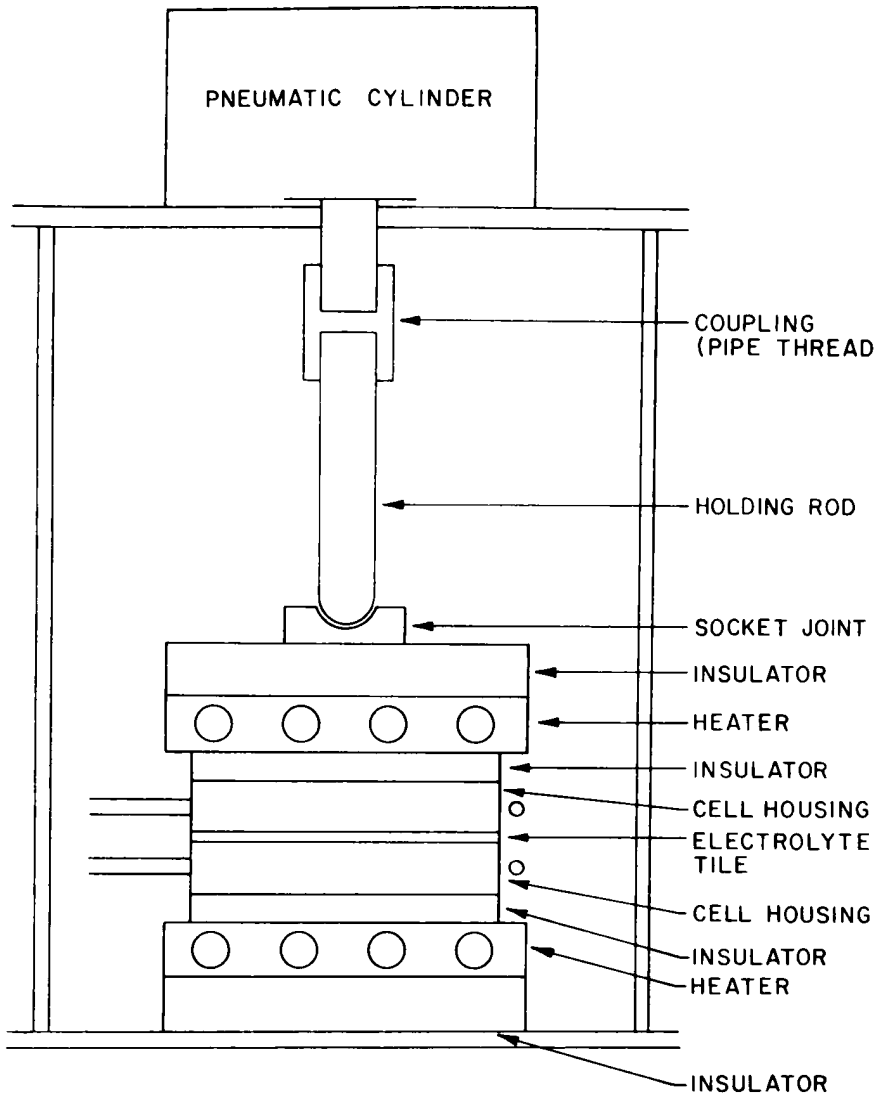

Fig. 18. Schematic of Fuel Cell Assembly

One cell (SQ-1) of the new configuration has been tested. Cross-leakage of reactant gases, caused by a crack in the electrolyte tile, prevented collection of meaningful polarization data, however. The cross-leakage was indicated by a low open-circuit voltage, which decreased further whenever a small back pressure (1 kPa) was imposed on either electrode. Also, analysis* of the anode exit gas stream showed 10-20% N_2. The fuel (anode) gas contains no N_2 but the oxidant (cathode) gas contains 57% N_2; therefore, cross-leakage of reactant gas from the cathode to the anode is indicated. Similar measurements on baseline cells of the CS-series generally showed less than 1% N_2, and the open-circuit voltage of baseline cells did not vary with

*Analysis performed by M. Homa, ANL Analytical Chemistry Lab.

the imposition of a small back pressure (1 kPa) on either electrode. The cause of the cross-leakage was determined (during post-test analysis) to be a crack (∿1-mm wide) in the electrolyte tile. Cracks of such magnitude have not previously been observed in post-test analyses of the CS-series cells. Thus, a number of experimental observations indicate that cross-leakage of reactant gas was occurring in Cell SQ-1, and this cross-leakage was caused by a crack in the electrolyte tile.

The cause of the crack in the electrolyte tile is uncertain, but a number of circumstances suggest that the tile was defective even before its use in Cell SQ-1. Because of vendor problems with the delivery of our 10.6 x 10.6-cm die, the tile had been pressed* as a disc, 17 cm in diameter. A square tile was then cut from this disc. The 17-cm disc was cracked on removal from the die, but a section of appropriate size remained intact for use. State-of-the-art tiles are not cracked when removed from the die.

We have just acquired a hardened steel die, shown schematically in Fig. 19, and pressing of electrolyte tiles in the die has begun. The die is of split design, which permits disassembly for removal of the tile. Temperature control during pressing has been excellent; the temperature measured in the side of the die has agreed with that measured in the center of the top punch to within ∿5°C. The first tile pressed was intact throughout, except for a broken corner. The break is believed to have occurred during removal of the tile from the die. Based on our experience to date, we do not expect problems in producing satisfactory tiles for use in the 10.6 x 10.6-cm cells.

*Pressing performed by The Institute of Gas Technology, Chicago, IL.

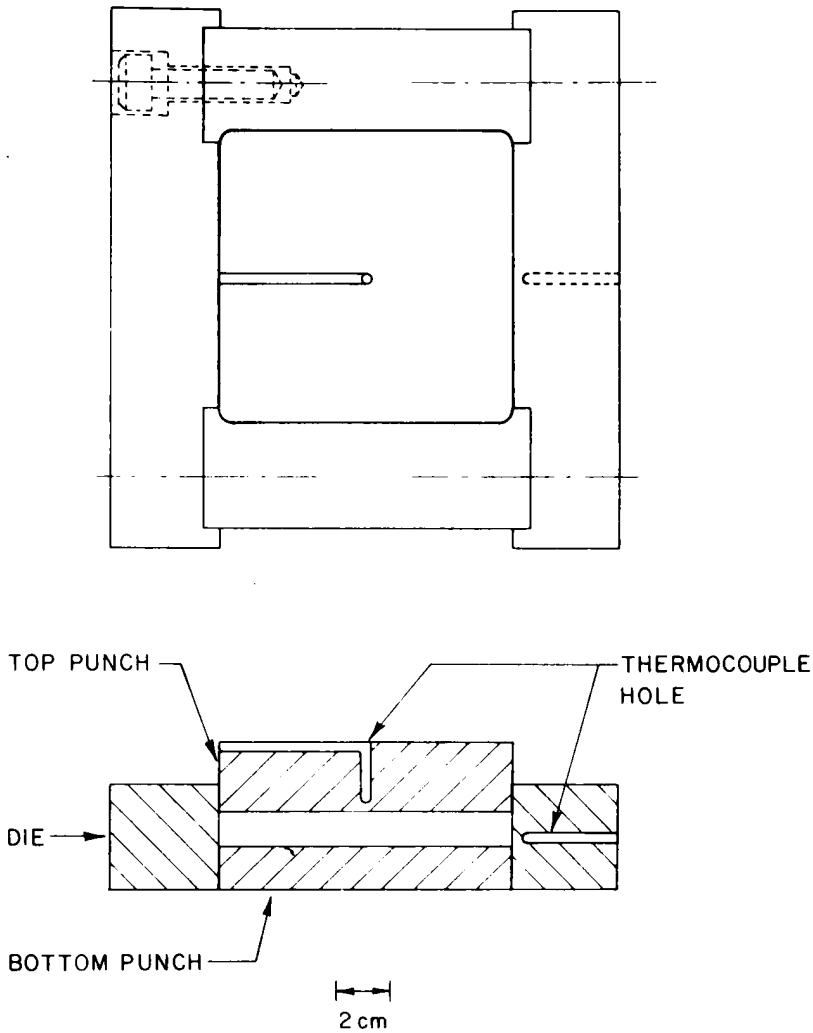

Fig. 19. Square Hot-Pressing Die

REFERENCES

1. N. N. Semenov, Izv. Sib. Otd. Akad. Nauk SSSR, Ser. Khim. Nauk 1, 156 (1967).

2. G. Sooki-Toth *et al.*, Hungarian Utility Patent Application 167 545, March 21, 1974.

3. R. E. Jaeger and T. J. Miller, Ceramic Bull. 53, 855 (1974).

Distribution for ANL-78-40

Internal:

E. G. Pewitt
J. P. Ackerman (25)
E. M. Bohn
L. Burris
F. A. Cafasso
L. Cuba
J. Harmon
R. O. Ivins
G. M. Kesser
K. Kinoshita
G. Kucera
A. Melton
P. A. Nelson (20)
J. W. Sim
R. K. Steunenberg
R. Swaroop
A. D. Tevebaugh
D. S. Webster
A. B. Krisciunas
ANL Contract File
ANL Libraries (5)
TIS Files (6)

External:

DOE-TIC, for distribution per UC-93 (171)
Manager, Chicago Operations Office
Chief, Chicago Patent Group
President, Argonne Universities Association
Chemical Engineering Division Review Committee:
  C. B. Alcock, U. Toronto
  R. C. Axtmann, Princeton U.
  R. E. Balzhiser, Electric Power Research Inst.
  J. T. Banchero, U. Notre Dame
  T. Cole, Ford Motor Co.
  P. W. Gilles, U. Kansas
  R. I. Newman, Allied Chemical Corp.
  R. M. Rosenblatt, Pennsylvania State U.
B. Baker, Energy Research Corp., Danbury, Conn.
T. R. Beck, Electrochemical Technology Corp., Seattle
P. Blum, Div. Power Systems, USDOE
D. Chatterji, General Electric Co., Schenectady
L. M. Ferris, Oak Ridge National Lab.
A. P. Fickett, Electric Power Research Inst.
V. Fiore, Gas Research Inst., Chicago
E. Gillis, Electric Power Research Inst.
J. Giner, Giner, Inc., Waltham, Mass.
J. W. Harrison, General Electric Co., Wilmington, Mass.
J. Huff, U. S. Army Mobility Equipment R&D Center
D. Johnson, Northwestern U.
J. M. King, United Technologies, Inc., South Windsor, Conn.
L. Marianowski, Inst. of Gas Technology, Chicago
L. Nanis, Stanford Research Inst.
J. J. Rasmussen, MERDI, Butte, Mont.
R. Selman, Illinois Inst. of Technology
G. Voelker, Div. Power Systems, USDOE
P. Weaver, Stanford Research Inst.
K. Wray, Physical Sciences, Inc., Woburn, Mass.
E. Yeager, Case Western Reserve U.
W. E. Wallace, Jr., Morgantown Energy Research Center

ARGONNE NATIONAL LAB WEST
3 4444 00023880 8